Received: 7 February 2024 | Revised: 19 June 2024 | Accepted: 23 July 2024

DOI: 10.1111/omi.12481

ORIGINAL ARTICLE

WILEY

Effects of fluid shear stress on oral biofilm formation and composition and the transcriptional response of *Streptococcus gordonii*

Brittany L. Nairn[1] | **Bruno P. Lima**[2] | **Ruoqiong Chen**[2] | **Judy Q. Yang**[3,4] | **Guanju Wei**[3,4] | **Ashwani K. Chumber**[2] | **Mark C. Herzberg**[2]

[1]Department of Biological Sciences, Bethel University, St. Paul, Minnesota, USA

[2]Department of Diagnostic and Biological Sciences, University of Minnesota, Minneapolis, Minnesota, USA

[3]Saint Anthony Falls Laboratory, University of Minnesota, Minneapolis, Minnesota, USA

[4]Department of Civil, Environmental, and Geo-Engineering, University of Minnesota, Minneapolis, Minnesota, USA

Correspondence
Brittany L. Nairn, Department of Biological Sciences, Bethel University, St. Paul, MN, USA.
Email: blima@umn.edu

Bruno P. Lima, Department of Diagnostic and Biological Sciences, University of Minnesota, Minneapolis, MN, USA.
Email: brittany-nairn@bethel.edu

Brittany L. Nairn and Bruno P. Lima are co-first authors.

Funding information
National Institute of Dental and Craniofacial Research, Grant/Award Numbers: R01 DE025618, K08 DE027705, R03 DE031337; National Science Foundation, Grant/Award Number: 2236497

Abstract

Biofilms are subjected to many environmental pressures that can influence community structure and physiology. In the oral cavity, and many other environments, biofilms are exposed to forces generated by fluid flow; however, our understanding of how oral biofilms respond to these forces remains limited. In this study, we developed a linear rocker model of fluid flow to study the impact of shear forces on *Streptococcus gordonii* and dental plaque-derived multispecies biofilms. We observed that as shear forces increased, *S. gordonii* biofilm biomass decreased. Reduced biomass was largely independent of overall bacterial growth. Transcriptome analysis of *S. gordonii* biofilms exposed to moderate levels of shear stress uncovered numerous genes with differential expression under shear. We also evaluated an ex vivo plaque biofilm exposed to fluid shear forces. Like *S. gordonii*, the plaque biofilm displayed decreased biomass as shear forces increased. Examination of plaque community composition revealed decreased diversity and compositional changes in the plaque biofilm exposed to shear. These studies help to elucidate the impact of fluid shear on oral bacteria and may be extended to other bacterial biofilm systems.

KEYWORDS
biofilms, oral, shear, *Streptococcus gordonii*

1 | INTRODUCTION

The oral microbiome comprises over 600 bacterial species and varies by location, host age, environment, diet, and other factors (Aas et al., 2005). Plaque biofilms are of particular interest due to their direct role in the development of dental caries and periodontitis, as well as other aspects of oral health, opportunistic infections, and cancer. The initiation of plaque formation relies on early colonizers such as *Streptococcus gordonii* and other streptococci (Baty et al., 2022). *Streptococcus gordonii* is a gram-positive oral commensal that contributes to plaque formation by binding salivary proteins (Aas et al., 2005) adsorbed onto the tooth surface and serving as a docking site to other members of the dental plaque community (Diaz et al., 2006). *Streptococcus gordonii* can

Abbreviations: CFD, computational fluid dynamics; DEGs, differentially expressed genes; DGE, differential gene expression; LDP, low-density proteins; OPM, oscillations per minute; OTUs, operational taxonomic units..

also bind human endothelial cells (Schollin, 1988) and accumulate on damaged heart valves leading to infective endocarditis. In these scenarios, bacterial attachment and subsequent biofilm formation occur and contribute ultimately to the pathogenesis of caries, periodontitis, and infective endocarditis.

While most biofilms are studied under static growth conditions, fluid flow is common to many microbial environments and has a particular impact on attachment and biofilm formation and maintenance. Fluid flow generates a shear force on the cells, resulting in numerous outcomes, depending on the microbe(s) and other environmental factors. In some cases, fluid flow can be beneficial, contributing to the distribution of public goods and structural organization of the biofilm community (Cremer et al., 2016; Kim et al., 2016). In other environments, fluid flow can increase microbial adhesion. Several studies have observed enhanced binding of bacterial cells under shear stress, termed shear-enhanced attachment, including *Escherichia coli*, *Pseudomonas aeruginosa*, *Staphylococcus epidermidis*, *S. aureus*, and *Borrelia burgdorferi* (Ebady et al., 2016; Lecuyer et al., 2011; Pappelbaum et al., 2013; Thomas et al., 2002; Weaver et al., 2011). Some species use specialized catch-bond adhesins, adhesins whose interactions with specific receptors are strengthened upon mechanical stress (Back et al., 2017; Ebady et al., 2016; Yakovenko et al., 2008). In *S. gordonii*, Hsa/GspB and CshA are thought to function as catch-bond adhesins with Hsa specifically contributing to shear-enhanced attachment (Back et al., 2017; Ding et al., 2010; Yakovenko et al., 2018). In all circumstances, microbes must respond and adapt to the mechanical influences of shear and turbulence.

Recent studies suggest a wide range of genes are altered in bacteria exposed to fluid shear stress, and the transcriptional response is dependent on the amount of shear, type of model, and organism (Alsharif et al., 2015; Dingemans et al., 2016; Rodesney et al., 2017; Sanfilippo et al., 2019; Thomen et al., 2017). One of these recent studies suggests that rheosensing, a type of mechanosensing independent of bis-(3'-5')-cyclic dimeric guanosine monophosphate (cyclic-di-GMP) by *P. aeruginosa*, is accomplished through the detection of flow rate but not mechanical force (Sanfilippo et al., 2019). Likely, the mechanosensing and/or gene regulation related to fluid shear forces are varied and further studies are required.

In the oral cavity, mastication, speaking, and other activities can generate the movement of saliva and hence exert fluid shear forces over plaque biofilms. At the tooth surface, it is estimated that shear stress generated by saliva is approximately 0.762 dyn/cm^2 (or 0.0762 Pa; Prakobphol et al., 1995). On the other hand, on heart valves, the location of infective endocarditis, fluid shear stress is estimated in the range of 20 to 80 dyn/cm^2 (Weston et al., 1999). Therefore, bacteria such as *S. gordonii* and certain other oral opportunistic bacteria must adapt to a wide range of shear stress conditions, yet little is known regarding the mechanisms by which *S. gordonii* and the oral microbiota members respond to shear forces.

Some studies have described the impact of fluid shear forces on oral biofilms, and findings largely suggest that at some threshold, shear stress will decrease biofilm biomass, biofilm strength, and alter the biofilm architecture of monospecies and multispecies oral biofilms (Christersson et al., 1988; Fernández et al., 2016; Paramonova et al., 2009; Saunders & Greenman, 2000; Sharma et al., 2005). Fluid shear forces also seem to affect community composition, with increased shear stress decreasing community diversity (Fernández et al., 2016). Conversely, shear-enhanced adhesion and subsequent increased biofilm biomass under shear forces have also been observed (Ding et al., 2010; Fernández et al., 2016; Yakovenko et al., 2018). Teasing out the differences in the effects of shear stress on bacteria is complicated by differences in model systems, degrees of fluid shear employed, bacterial species studied, and other growth conditions.

Here, we describe a simple, adaptable, and inexpensive model of shear utilizing a linear rocker to investigate questions of *S. gordonii* biofilm formation, growth, and transcriptional response. We also apply this model to an ex vivo dental plaque biofilm community to probe changes in multispecies biofilm formation and community composition in response to shear forces. We show that overall, increasing shear forces reduce *S. gordonii* biofilm biomass with minimal impact on bacterial growth, accompanied by changes in its transcriptional profile. Plaque biofilms also showed reduced biomass with increased shear force, accompanied by changes in the community composition.

2 | MATERIALS AND METHODS

2.1 | Bacterial strains and growth conditions

Streptococcus gordonii DL1 was grown in Bacto brain heart infusion (BHI) broth or on BHI agar plates (Difco) at 37°C in 5% CO_2. The ex vivo plaque community was grown in modified Shi medium (75% sterile human saliva and 25% SHI medium; Saavedra et al., 2022) at 37°C in 5% CO_2.

2.2 | Rocker model of fluid shear

For both *S. gordonii* and the plaque community biofilms, to generate fluid flow, a linear rocker model 55 rocking shaker (Reliable Scientific Inc.) was placed in an incubator at 37°C in 5% CO_2. Culture plates were placed at the center of the rocker at various rocker settings to generate the designated velocity as measured by oscillations per minute (OPM), that is, a complete back-and-forth motion of the rocker shelf. For comparison, an identical plate was placed on the incubator shelf, that is, static conditions.

2.3 | COMSOL numerical simulation

We simulated the flow within culture plates situated on a rocker in three dimensions using computational fluid dynamics (CFD) finite-element simulation software, COMSOL Multiphysics 5.5. The 3D plate

was assumed to be 3.5-cm wide and 1-cm tall, and the water depth was 0.25 cm. We simplified the motion of the rocking shaker as a 3° × sin (ωt), where the angular velocity $\omega = 2\pi/T$ with T representing the period of the rotating cycle. The rotating periods T = 12, 6, 4, 3, 2.4, and 2 s correspond to 5, 10, 15, 20, 25, and 30 OPM of the rocker, respectively.

In our simulations, we considered that the flow in the culture plates was a two-phase laminar flow and conducted the CFD simulation using the phase field method (Akhlaghi et al., 2013; COMSOL, 2015). We did not consider the turbulence effect as the calculated Reynolds number is around 80 ($Re = \rho UL/\mu$, where ρ is the water density, U = 0.04 m/s is the maximum velocity, L is the water depth, and μ is the dynamic viscosity of water). In the simulation, the Navier–Stokes equation was numerically solved for flow velocity, assuming no-slip boundary conditions on all solid boundaries. The upper boundary is characterized as an open boundary. The time-dependent forms of the equations for laminar flow are the momentum equation (Equation 1) and the continuity equation (Equation 2).

$$\rho\frac{\partial u}{\partial t} + \rho\left(u \cdot \nabla\right)u = \nabla \cdot \left[-pI + \mu\left(\nabla u + \left(\nabla u\right)^T\right)\right] + F + \rho g, \quad (1)$$

$$\rho\nabla \cdot \left(u\right) = 0, \quad (2)$$

where ρ is the fluid density, u is the velocity, p is the pressure, I is the identity matrix, and F is the volume force vector.

The interface was tracked by the phase field method (Equations 3 and 4).

$$\frac{\partial \phi}{\partial t} + u \cdot \nabla\phi = \nabla \cdot \frac{\gamma\lambda}{\varepsilon^2}\nabla\psi, \quad (3)$$

$$\psi = -\nabla \cdot \varepsilon^2\nabla\phi + \left(\phi^2 - 1\right)\phi + \left(\frac{\varepsilon^2}{\lambda}\right)\frac{\partial f}{\partial \phi}, \quad (4)$$

where ϕ is the phase field variable, λ is the mixing energy density, ε is the interface thickness, γ is related to ε through $\gamma = \chi\varepsilon^2$ where χ is the mobility tuning parameter, and f is the body force.

For the simulation setup, the initial phase field values were set to $\phi = -1$ for fluid one (air) and $\phi = 1$ for fluid two (water). The simulation was conducted over a total time of 10 s, with results output every 0.1 s. The user-defined mesh consisted of 170,485 domains, with an average element quality of 0.68. The temperature was held constant at 293.15 K.

Shear stress distributions within the water phase were calculated based on the velocity profiles (shear stress $\tau = \mu\frac{du}{dy}$, μ is the dynamic viscosity, u is the velocity) in COMSOL. The spatially averaged shear stress at the bottom ($\tau_{\text{bottom-avg}}$) was calculated by averaging shear stress values at the bottom surface of the plate. Furthermore, the time-averaged shear stress ($\tau_{\text{time-avg}}$) was calculated as the average of bottom wall shear stress over the entire simulation duration of 10 seconds. The $\tau_{\text{time-avg}}$ exhibits a linear relationship with the rocker velocity.

2.4 | Saliva collection and preparation for coating plates

Stimulated saliva was collected and pooled from at least three healthy volunteers using protocols that were approved by the Institutional Review Board from the University of Minnesota (STUDY00016289). Saliva was collected by expectoration into tubes on ice. These samples were centrifuged for 10 min at 4°C at 1000 × *g* (Beckman SX4750 rotor) to remove large debris and bacterial aggregates. Following supernatant collection, the planktonic bacteria were pelleted by centrifugation at 15,000 × *g* for 20 min at 4°C and supernatants were again collected and saved for coating plates.

2.5 | Biofilm formation

Following overnight culture, bacteria were inoculated at 1:100 v:v in BHI or Shi media in tissue culture-treated plates (Costar), and incubated at 37°C and 5% CO_2 for 24 h. For some experiments, prior to inoculation, plates were coated with saliva or salivary fractions as described below. Following incubation under the designated static or flow conditions, biofilm biomass was measured by crystal violet (CV) staining. To each well was added 0.1% CV solution and plates incubated at room temperature for 15 min. Plates were gently washed four times with phosphate buffered saline (PBS). Plates were air dried for 1 min and then acidified ethanol (4% 1N HCl/96% EtOH) was added to each well. Samples were mixed by pipetting up and down, and the CV–ethanol mix was transferred to a flat-bottomed, polystyrene 96-well plate and measured the absorbance at 570 nm using the ChroMate 4300 microplate plate reader (Awareness Technology).

For experiments utilizing saliva, saliva prepared as described above was added to each well to cover the bottom surface and incubated with rocking for 1 h at room temperature. Unbound saliva was then removed, and the plates and bound saliva were sterilized by exposure to UV irradiation for 15 min (Spectroline UV Crosslinker FB-UVXL-1000; Spectronics) prior to biofilm inoculation.

For experiments utilizing MUC5B and low-density proteins (LDP), fractions were provided by Claes Wickström at Malmö University, Malmö, Sweden, after purification from human saliva as previously reported (Kindblom et al., 2012). The fractions were used to coat wells for biofilm assays at concentrations approximating their native proportions in human saliva. Plates were incubated with rocking for 1 h at room temperature when the salivary solution was gently aspirated.

2.6 | Streptococcus gordonii growth measurements

Following overnight culture in BHI, *S. gordonii* was inoculated at 1:100 v:v in BHI into tissue culture-treated plates (Costar) and incubated at 37°C and 5% CO_2 for 24 h. For some experiments, prior to inoculation, plates were coated with saliva as done for biofilm formation assays. Following incubation under the designated static or flow conditions,

adherent cells were scraped using sterile wooden applicators, and all cells (planktonic and removed adherent cells) were mixed by a pipette.

To quantify bacteria by turbidity, cells were diluted 1:1 in BHI media in a cuvette, and the absorbance at 600 nm was collected using a BioMate 160 UV-Visible spectrophotometer (Thermo Scientific).

To quantify bacteria based on adenosine triphosphate (ATP) quantification, the BacTiter-Glo Microbial Cell Viability Assay (Promega) was used following the manufacturer's instructions. Specifically, 100 µL of cells were added to wells of a white, flat-bottomed 96-well plate followed by 100 µL of BacTiter-Glo Reagent. Contents were mixed briefly on a rocker and incubated for 5 min at room temperature. Luminescence was measured using a SpectraMax iD3 plate reader (Molecular Devices).

2.7 | Total RNA purification, RNAseq, and quantitative RT-PCR

To assess gene expression by sessile cells, the biofilms were washed with sterile PBS and scraped from the surface to harvest. Cells were then resuspended in 500 µL of TRIzol reagent (Ambion) and lysed by bead beating as described previously (Nobbs et al., 2007). Following lysis, total RNA was purified as previously (Hall et al., 2019).

RNA sequencing was performed at the University of Minnesota Genomic Center as described (Hall et al., 2019). Differential gene expression (DGE) analysis was performed in Geneious Prime using DESeq2 within R. DGE lists were generated using a differential expression log2 ratio > 1.0 or < −1.0. An adjusted *p*-value of ≤0.01 was considered significant.

For quantitative, reverse transcription PCR (RT-PCR), total RNA was converted to cDNA using the ProtoScript II first-strand cDNA synthesis kit (New England Biolabs) with random hexamer primers according to the manufacturer's protocol. For quantitative PCR, 1:10 dilutions of cDNA were used in reactions with Maxima SYBR Green/ROX qPCR master mix (Thermo Scientific) according to the manufacturer's protocol. A two-step cycling program was utilized, which included an initial denaturation at 95°C for 10 min followed by 40 cycles of 95°C for 15 s (denaturation) and 60°C for 1 min (annealing/extension) using the Mx3000 real-time PCR system (Stratagene). Relative gene expression was calculated using the threshold cycle (ΔΔCt) method.

2.8 | DNA extraction and 16S rRNA sequencing

For community composition analysis, ex vivo plaque community was grown as described above under static and shear conditions. The biofilms were washed with sterile PBS and scraped from the surface to harvest. Genomic DNA was isolated using the DNeasy PowerSoil Kit (QIAGEN) according to the manufacturer's instructions. The DNA concentration was determined using Qubit (Invitrogen), and total genomic DNA (~3 µg) was submitted for Illumina MiSeq sequencing of the V3-V4 hypervariable regions of the 16S rRNA at SeqCenter. Samples were prepared using Zymo Research's Quick-16S kit. Following clean-up and normalization, samples were sequenced on a V3 MiSeq 622cyc flow cell to generate 2 × 301 bp PE reads. Quality control and adapter trimming were performed with bcl-convert (Illumina, 2020). Sequences were imported into Qiime2 (Bolyen et al., 2019) for subsequent analysis. Primer sequences were removed using Qiime2's cutadapt plugin (Martin, 2011). Sequences were denoised using Qiime2's dada2 plugin (Callahan et al., 2016). Denoised sequences were assigned operational taxonomic units (OTUs) using the Silva 138 99% OTUs full-length sequence database and the VSEARCH (Rognes et al., 2016) utility within Qiime2's feature-classifier plugin. OTUs were then collapsed to their lowest taxonomic units, and their counts were converted to reflect their relative frequency within a sample.

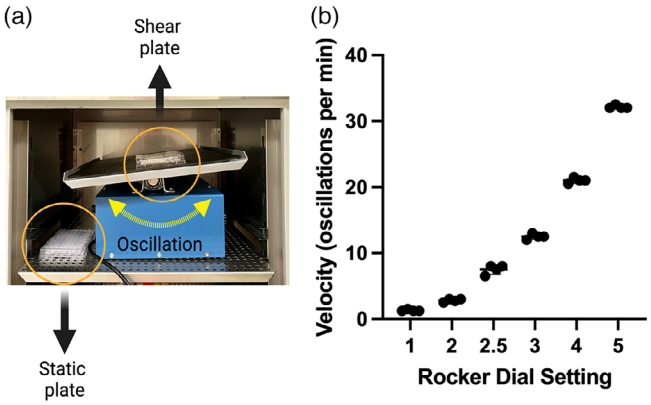

FIGURE 1 Use of a linear rocker to generate fluid shear. (a) Image of the rocker used to generate fluid shear. Arrows designate the measure of one oscillation used to assess velocity. (b) Measurement of rocker velocity by rocker dial setting. $N = 3$.

2.9 | Data availability

The RNA-seq data are available at Geo accession number GSE202049. The microbiome data have been uploaded to NCBI and are available under BioProject number PRJNA1070294.

3 | RESULTS

3.1 | A rocker model of fluid shear

We developed a model of fluid shear that utilizes a linear rocker. It is conducive to use with various culturing dishes and microbial species. We measured rocker velocity through an assessment of the number of OPM or a complete back-and-forth of the rocker shelf (Figure 1a). This allowed us to correlate the rocker dial settings to a specific velocity as shown in Figure 1b. For static growth conditions, culture plates are placed on the incubator shelf. In culture systems with liquid media, the flow of the media is arguably similar in velocity to the rocker and generates a correlative amount of fluid shear force on the bacteria.

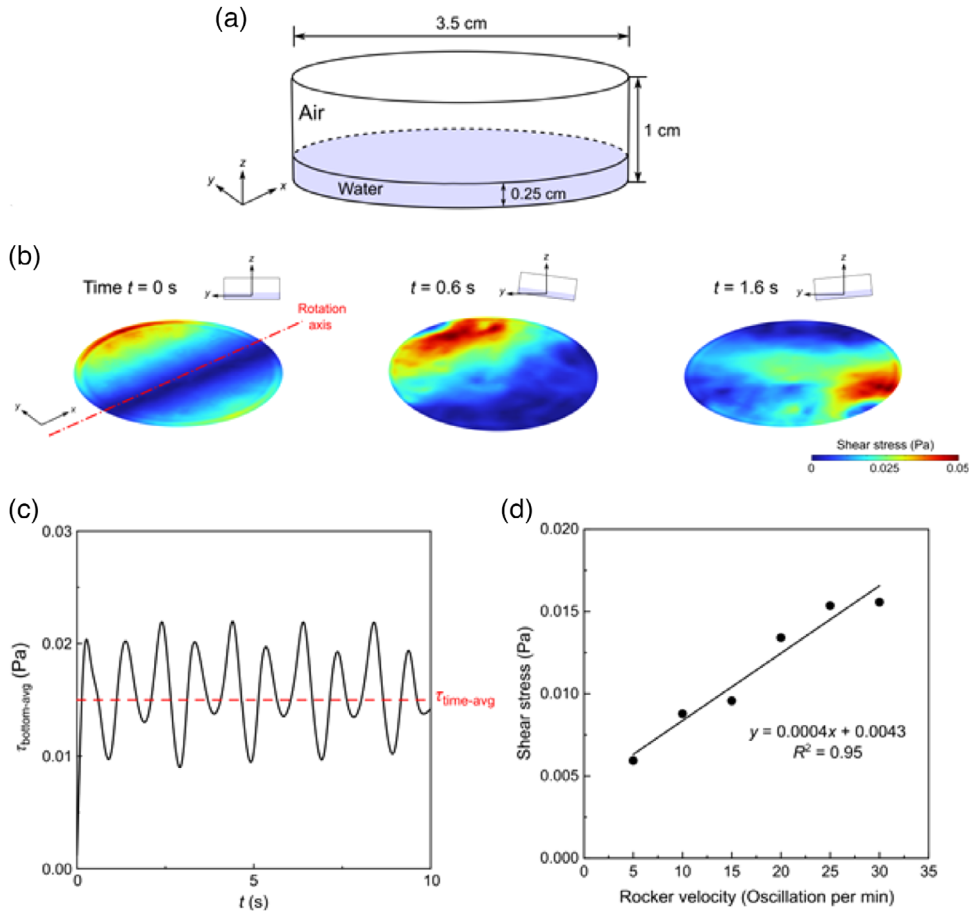

FIGURE 2 Computational fluid dynamics and calculation of fluid shear forces. (a) The geometry of the simulated 3D circular well. The well was 3.5-cm wide and 1-cm tall and the water depth was 0.25 cm. (b) Shear stress distribution within the fluid phase on the bottom plane at different times with a rocker velocity of 30 oscillations per minute (OPM). (c) Spatially averaged shear stress ($\tau_{bottom\text{-}avg}$) at the bottom plotted over time with a rocker velocity of 30 OPM. The time-averaged shear stress ($\tau_{time\text{-}avg}$) was defined as the average of bottom wall shear stress over the entire simulation duration of 10 s. (d) The time-averaged shear stress ($\tau_{time\text{-}avg}$) as a function of the rocker velocity.

To specifically calculate the fluid shear force experienced by the biofilm bacteria, we simulated the flow within culture plates using CFD finite-element simulation software. In our simulations, we considered that the flow in the culture plates was a two-phase laminar flow and conducted the CFD simulation using the phase field method (Akhlaghi et al., 2013; COMSOL, 2015). We conducted calculations to assess the Reynolds number associated with the flow induced by the back-and-forth motion of the rocker, which indicates that the Reynolds number is on the order of 80, falling within the range characteristic of laminar flow. This suggests that turbulence is not a significant factor in the flow generated by our rocker model. In the simulation, the Navier–Stokes equation was numerically solved for flow velocity, assuming no-slip boundary conditions on all solid boundaries. The upper boundary is characterized as an open boundary. The geometry of the simulated 3D circular well was defined as 3.5-cm wide and 1-cm tall, and the water depth was 0.25 cm (Figure 2a). Figure 2b shows shear stress distribution within the fluid phase on the bottom plane at different times with a rocker velocity of 30 OPM. We calculated spatially averaged shear stress ($\tau_{bottom\text{-}avg}$) at the bottom plotted over time. Figure 2c shows these values at a rocker velocity of 30 OPM. The time-averaged shear stress ($\tau_{time\text{-}avg}$) was defined as the average of bottom wall shear stress over the entire simulation duration of 10 s. We calculated the time-averaged shear stress as a function of the rocker velocities (Figure 2d). These time-averaged shear stress values show a linear relationship with velocity.

3.2 | Effects of fluid shear on *S. gordonii* biofilm formation

To evaluate the effects of fluid shear on *S. gordonii* biofilms, bacteria were grown in 12-well plates under static conditions or on the rocker set to six increasing rocker velocities. Biofilm biomass was assessed by crystal violet (staining of adherent cells following 24 h of growth. As shown in Figure 3a, as rocker velocity increased, biofilm biomass decreased, with one exception, at 1.25 OPM, where biofilm biomass slightly increased, though this difference was not statistically significant. The crystal violet staining also revealed a unique biofilm

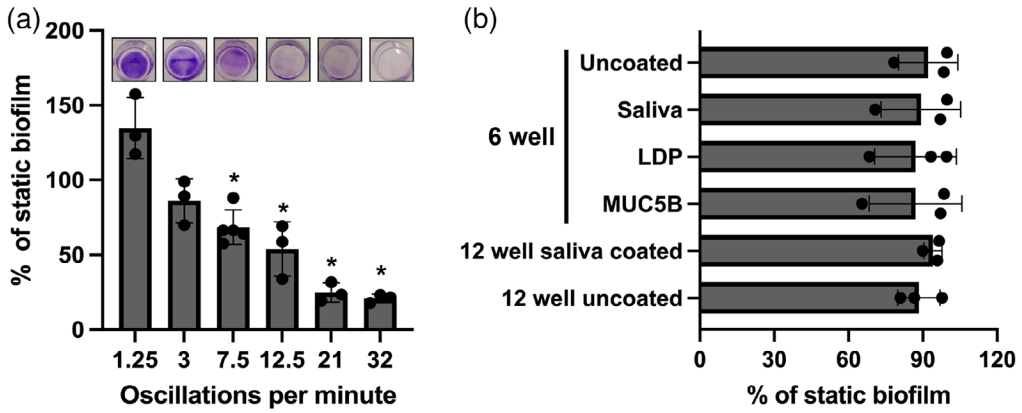

FIGURE 3 Biofilm formation of *Streptococcus gordonii* under fluid shear. (a) *Streptococcus gordonii* biofilm biomass following growth in BHI in 12-well plates for 24 h. Data are reported as the mean ± SD percentage of static biofilm biomass from ≥3 separate experiments. Representative image of a well under each condition following crystal violet staining is shown above the associated bar. *p-value ≤ 0.05 as determined by Student's t-test comparing each velocity to static = 100; (B) *S. gordonii* biofilm biomass following growth in BHI in 12-well or 6-well plates either uncoated or coated with saliva, MUC5B or low-density proteins (LDP) following incubation of 24 h either under static conditions or at a velocity of 3 OPM. Data are reported as the mean ± SD percentage of static biofilm biomass from ≥3 separate experiments.

structure with increased density in linear format across the center of the well, when the biofilm was incubated under moderate velocities. This structure likely reflects the movement of the media through the well and correlates with an area of decreased shear stress based on our simulation (Supporting Information Figure S1).

We also evaluated the biomass of cells grown in 6-well plates and on saliva and two fractions of saliva, MUC5B and low density proteins (LDP). One of the dominant mucins in saliva is MUC5B, a component of the salivary pellicle that coats the teeth and serves as a substrate for bacterial adhesion in the oral cavity (Kindblom et al., 2012; Siqueira et al., 2007; Yao et al., 2003). Using ultracentrifugation, saliva can be partitioned into a MUC5B-enriched fraction and a second fraction enriched for the remaining LDP including MUC7 and gp340, two other glycoproteins involved in bacterial adherence (Jakubovics et al., 2005; Kindblom et al., 2012; Ruhl et al., 2004). Figure 3b shows biomass quantification demonstrating that plate and substrate largely do not impact biofilm formation under shear at the tested velocity (3 OPM).

3.3 | Effects of fluid shear on *S. gordonii* growth

It is possible that the fluid shear could limit nutrient accessibility and impact bacterial growth, ultimately affecting biofilm density, as has been previously observed (Kostenko et al., 2010; Liu & Tay, 2002). Thus, to assess whether the decrease in biofilm biomass was the result of a decrease in the overall growth of bacteria, we evaluated total biomass of both biofilm and planktonic bacteria by OD_{600nm} and viable cell numbers by ATP measurements. Low, moderate, and high OPM speeds were used and compared to static conditions. Biofilms were grown on either uncoated or saliva-coated plates. For biomass, no statistically significant difference was observed in OD_{600} values between static and shear conditions, regardless of whether the plate was uncoated or coated with saliva (Figure 4a). For cell viability, luminescence values quantifying the amount of ATP produced corresponds to viable cells, with a log fold-change in luminescence roughly equivalent to a log fold-change in cell number of *S. gordonii* (Figure 4d). At low and mid OPM, no changes in luminescence were observed; however, at the high velocity, a two-log reduction in luminescence was detected (Figure 4b,c). The same results were obtained for both uncoated and saliva-coated plates. These data suggest that the decrease in biofilm biomass under fluid shear is likely not due to an overall decrease in cell growth or viability until higher velocities and greater shear forces are applied.

3.4 | Streptococcus gordonii gene expression under fluid shear

While *S. gordonii* biofilm biomass decreases as shear forces increase, measurable biofilms are formed throughout the tested rocker velocities, suggesting an active response to the fluid flow. In other words, *S. gordonii* is likely sensing fluid flow or shear forces and altering its gene expression. Therefore, we assessed the *S. gordonii* transcriptome in response to a moderate level of fluid shear forces (7.5 OPM) at a point when biofilm formation is only partly affected, and growth is not changed, suggesting an active and productive response by *S. gordonii*. Since our previous data suggest that *S. gordonii* cells can sense interaction with a MUC5B-coated surface (Lima et al., 2019), we evaluated the gene expression of biofilms growing on MUC5B and LDP fractions of saliva. *Streptococcus gordonii* was grown on both MUC5B- or LDP-coated plates for 24 h under static conditions and at a rocker velocity of 7.5 OPM. Following RNA isolation, RNAseq was used to evaluate the transcription profile. To identify differentially expressed genes (DEGs) in response to fluid flow, our cutoff values were a fold change of 2 and a p-value ≤ 0.01.

On MUC5B-coated surfaces, 162 genes were differentially expressed in shear, compared to static conditions, whereas 76 genes

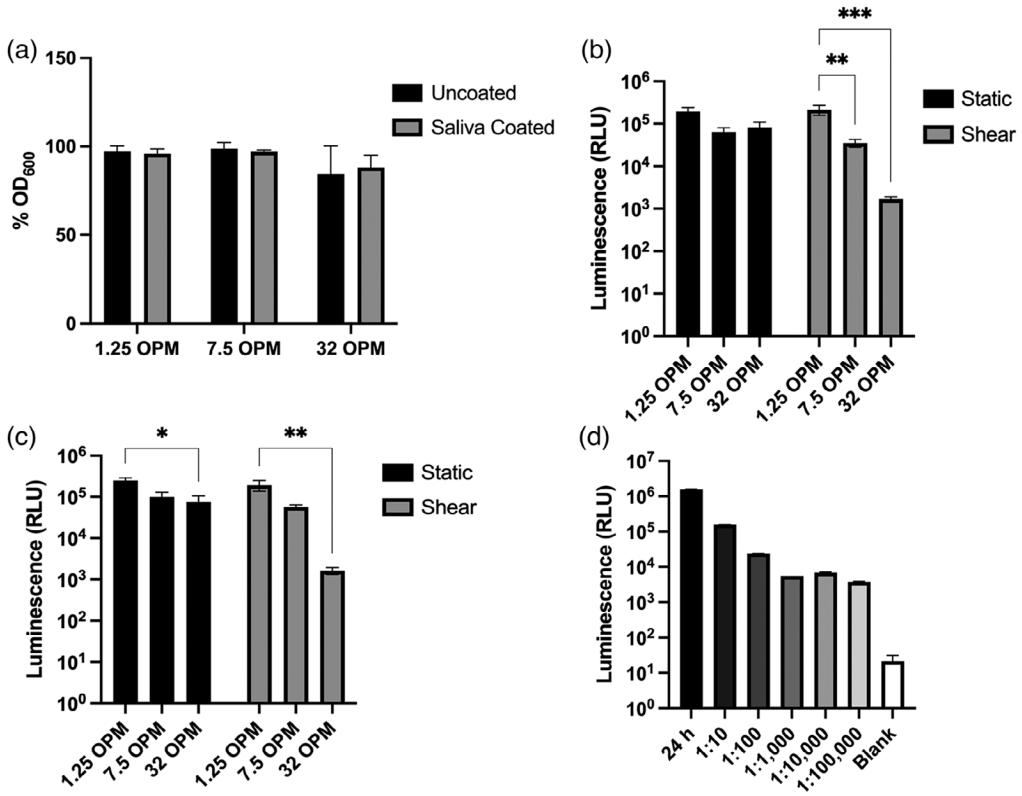

FIGURE 4 Growth of *S. gordonii* under fluid shear. (a) *Streptococcus gordonii* growth as measured by optical density at 600 nm from collected planktonic plus biofilm cells. Bacteria were grown in BHI on uncoated or saliva-coated 12-well plates for 24 h under static conditions or rocker velocities of 1.2, 7.5, or 32 OPM. Data are reported as the mean ± SD percentage of static OD600 from ≥3 separate experiments. (b) *Streptococcus gordonii* growth as measured by ATP quantification from collected planktonic plus biofilm cells. Bacteria were grown in BHI on uncoated 12-well plates for 24 h under static conditions or rocker velocities of 1.25, 7.5, or 32 OPM. Data are reported as mean ± SD luminescence from ≥3 separate experiments. **p*-value ≤ 0.05 as determined by Student's *t*-test comparing each velocity to static. (c) *Streptococcus gordonii* growth as measured by ATP quantification from collected planktonic plus biofilm cells. Bacteria were grown in BHI on saliva-coated 12-well plates for 24 h under static conditions or rocker velocities of 1.25, 7.5, or 32 OPM. Data are reported as mean ± SD luminescence from ≥3 separate experiments. **p*-value ≤ 0.05 as determined by Student's *t*-test comparing each velocity to static = 100. (d) ATP quantification of 10-fold serial dilutions of *S. gordonii* grown in BHI. Data are reported as mean ± SD luminescence.

were differentially expressed on LDP-coated surfaces. Of those 238 DEGs, 50 were differentially expressed regardless of how the plates were coated, that is, either MUC5B or LDP (Figure 5, Supporting Information Tables S1 and S2).

Of the 162 DEGs in MUC5B-grown biofilm, 34 were up-regulated under shear, while 128 were down (Figure 5a). Gene ontology analysis revealed an enrichment in genes that code for translation-related proteins under shear conditions and a decrease in genes that encode proteins involved in multiple sugar metabolism pathways (Figures 5b,c). For LDP-grown biofilms, 12 genes were more abundantly expressed under shear, while 54 were down-regulated (Figure 5d). Static LDP conditions seemed to favor the expression of genes linked to polysaccharide metabolism, such as glycogen and glucans (Figure 5e). Of the 50 genes differentially expressed regardless of the plate-coating substrate, only four were up-regulated under shear: *rplE* and *rpsQ*, which encode ribosomal proteins; *SGO_RS02250*, which encodes a putative transcriptional regulator; and *glmS*, which encodes a glucosamine-fructose-6-phosphate aminotransferase. Gene ontology analysis showed enrichment for genes involved in polysaccharide metabolism among the genes down-regulated under shear conditions in both MUC5B- and LDP-coated plate biofilms. The full list of DEGs is shown in Supporting Information Tables S1 and S2.

We selected four DEGs from the list of genes differentially expressed regardless of the coating substrate (*abpB*, *SGO_RS01315*, *SGO_RS02250*, and *SGO_RS06940*) and included two genes that encode surface adhesin proteins: *mbpA*, which we previously showed helps *S. gordonii* sense interaction with MUC5B (Lima et al., 2019), and *hsa*, which encodes a catch-bond adhesin contributing to shear-enhanced attachment (Ding et al., 2010; Yakovenko et al., 2018), to evaluate gene expression by quantitative RT-PCR (Table 1, Figure 6). These data largely confirm the trends related to differential expression seen in the RNAseq (Tables 1, S1, and S2). Additionally, the same expression pattern was seen in cultures grown on saliva-coated plates, further suggesting changes specific to shear and independent of substrate.

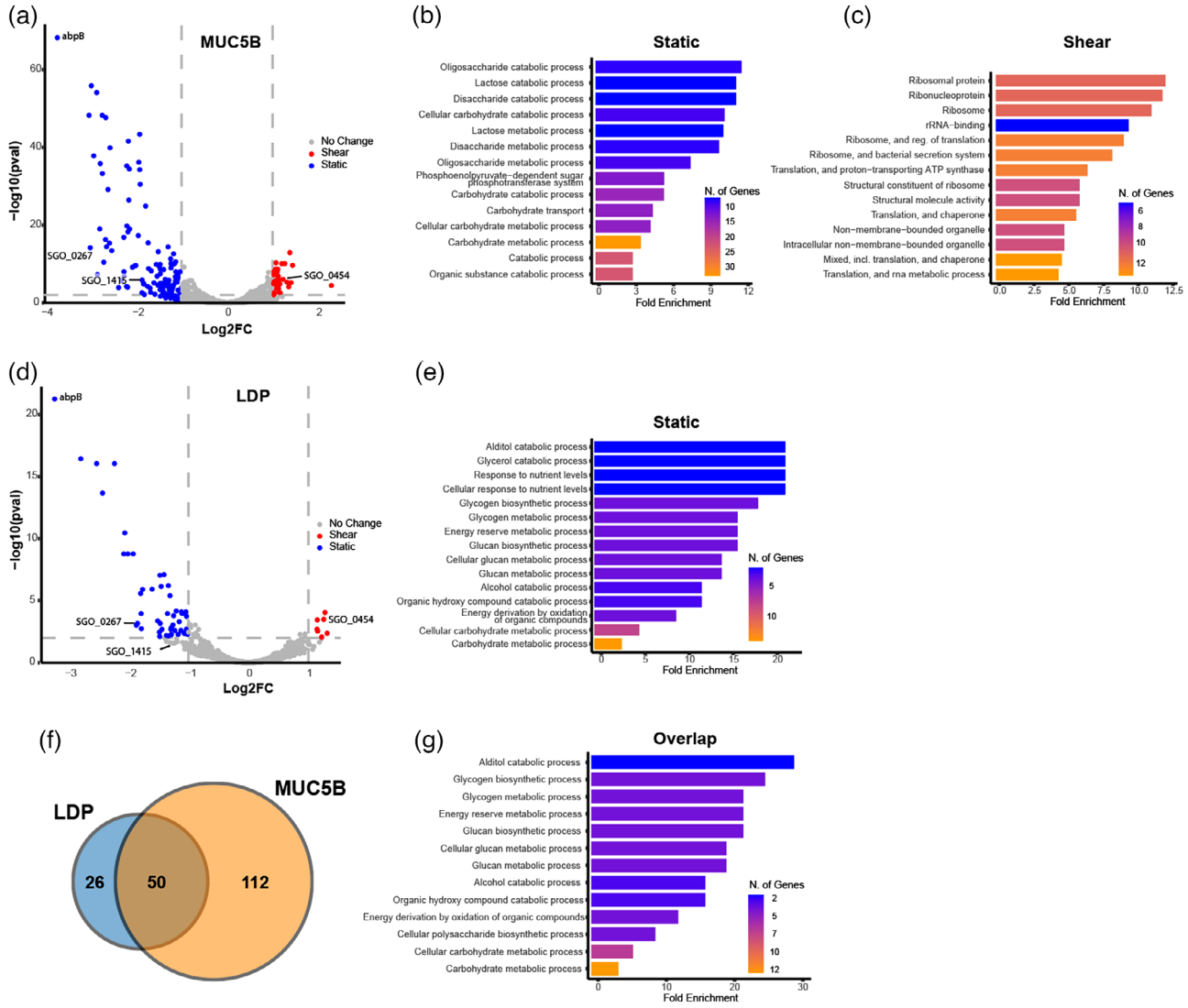

FIGURE 5 Transcriptional profile of *S. gordonii* exposed to fluid shear stress. Volcano plot of genes differentially expressed (genes with ≥ 2 Log10 *p*-value and Log2 fold change ≥ 1 or ≤ −1) between shear (red) and static (blue) conditions of *S. gordonii* biofilms grown on (a) MUC5B or (d) LDP, each $N = 3$. Gene ontology analysis of DEGs more abundantly expressed under (b) static or (c) shear conditions from biofilms grown on MUC5B. (e) Given the low number of genes upregulated under shear for biofilms grown on LDP, gene ontology analysis was performed only for genes more abundantly expressed under static conditions. (f) Venn diagram of the number of *S. gordonii* DEGs in response to shear stress on biofilms grown on MUC5B (orange) and LDP (blue), or common to both substrates (overlap). (g) Gene ontology analysis of DEGs regardless of substrate.

TABLE 1 List of genes selected for quantitative RT-PCR analysis, their RNAseq fold-changes, and annotations.

Fold-change MUC5B	Fold-change LDP	Gene name and description or annotation
1.256	1.4047	*hsa*; hemagglutinin, adhesin; entire synthetic operon
1.26	1.0029	*mbpA*; *SGO_RS03480* (old locus: *SGO_0707*); adhesin
2.344	2.3859	*SGO_RS02250* (old locus: *SGO_0454*); YebC/PmpR family transcriptional regulator
−13.25	−9.3739	*abpB*; C69 family dipeptidyl-dipeptidase
−3.643	−2.392	*SGO_RS06940* (old locus: *SGO_1415*); X-prolyl dipeptidyl-aminopeptidase
−8.03	−3.5995	*SGO_RS01315* (old locus: *SGO_0267*); polyamine/amino acid transporter PotE

Abbreviation: LDP, low-density proteins.

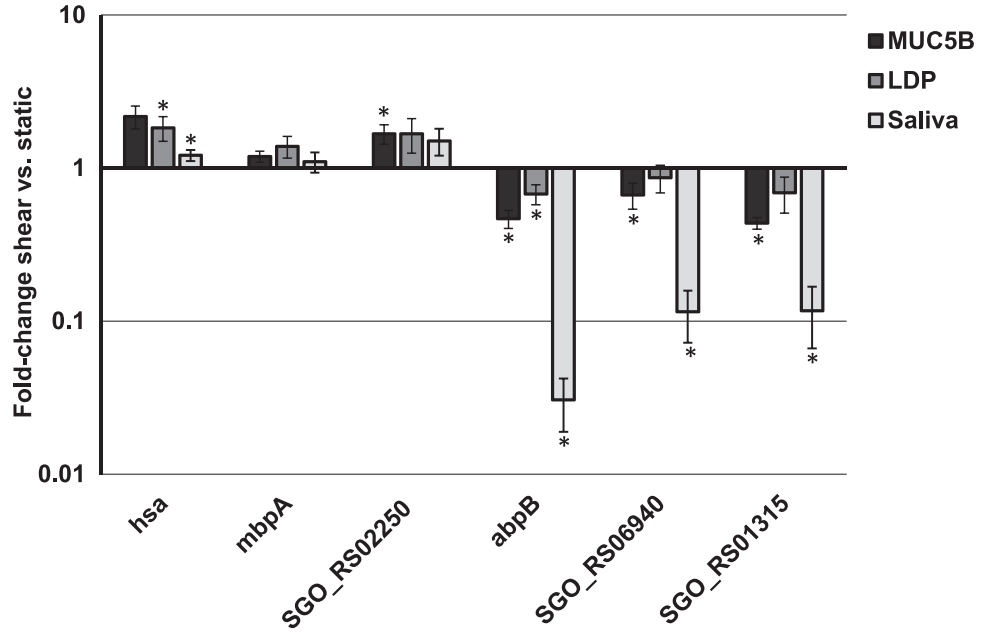

FIGURE 6 Evaluation of selected genes by quantitative RT-PCR. Seven genes were evaluated by quantitative RT-PCR in *S. gordonii* grown under the same conditions as RNAseq experiments, including on saliva-coated plates. Data are reported as mean ± SD fold-change under fluid shear conditions, compared to static conditions from ≥3 separate experiments. **p*-value ≤ 0.05 as determined by Student's *t*-test comparing the average fold-changes from each of the three experiments to 1.0 (unchanged).

3.5 | Effect of fluid shear on ex vivo plaque community biofilm formation and community composition

Streptococcus gordonii is one of the approximately 700 bacterial species found in the human oral cavity. Given its ability to readily bind to the salivary pellicle adsorbed onto the tooth surface, *S. gordonii* is thought to play an important role in dental plaque development. Because shear forces affected *S. gordonii* biofilms and its transcriptional profile, we hypothesized that fluid shear forces should also have a significant impact on the formation and composition of dental plaque. To test this hypothesis, we exposed our ex vivo dental plaque model to different fluid shear forces generated by our rocker model. Different from what we observed with *S. gordonii* single species biofilms, we did not observe any increase in biofilm biomass at the lowest OPM velocity, and the biofilm biomass produced by our in vitro plaque community model rapidly decreased with increased OPM velocity as compared to the static biofilm (Figure 7a).

To determine if shear forces affected the composition of our in vitro dental plaque model, we collected biofilms that were exposed to fluid flow at 1.5, 7.5, and 21 OPM, as well as their static biofilm controls. The genomic DNA was extracted and submitted for 16S rRNA sequencing analysis of the V3-V4 regions. The 1.5 OPM had no effect on the community composition of our ex vivo plaque community model, compared to the static control. However, the biofilms exposed to 7.5 and 21 OPM were composed of a significantly different bacterial community, compared to their static control, as evidenced by the decrease in Shannon index values (Figure 7b). In particular, as shown in Figure 7c, we observed an increase in the proportion of *Aggregatibacter*, *Haemophilus*, and *Eikenella*, and a decrease in *Porphyromonas*, *Parvimonas*, *Fusobacterium*, and *Peptostreptococcus*. No significant difference in community diversity and composition was observed when comparing 7.5 and 21 OPM (Figure 7b,c).

4 | DISCUSSION

Here, we investigated the role of fluid shear on biofilms formed by oral bacteria. We first investigated how single-species biofilms of *S. gordonii* were impacted by shear by assessing biomass, metabolic activity, and transcriptional response. We then used our ex vivo dental plaque model to assess the impact of shear forces on multispecies biofilm biomass and community composition.

Using our rocker model of fluid shear, we were able to incrementally alter fluid flow over bacteria grown on varying substrates and vessels (Figure 1). We were also able to calculate fluid shear stress averaged over the circular well surface as a function of velocity and over time using CFD (Figure 2). At 30 OPM, the time-averaged shear stress ($\tau_{\text{time-avg}}$) at the bottom is 0.02 Pa, with a local maximum shear stress of 0.06 Pa. While studies vary, these values are comparable to those used in other microfluidic models (Ding et al., 2010; Fernández et al., 2016; G. Wei & Yang, 2023). Importantly, the range of shear force values generated by the rocker is relatively close to the estimated 0.0762 Pa in the oral cavity (Prakobphol et al., 1995). Being that these calculations are averages, the shear stress would vary across different areas within the wells, and our results indicate that shear

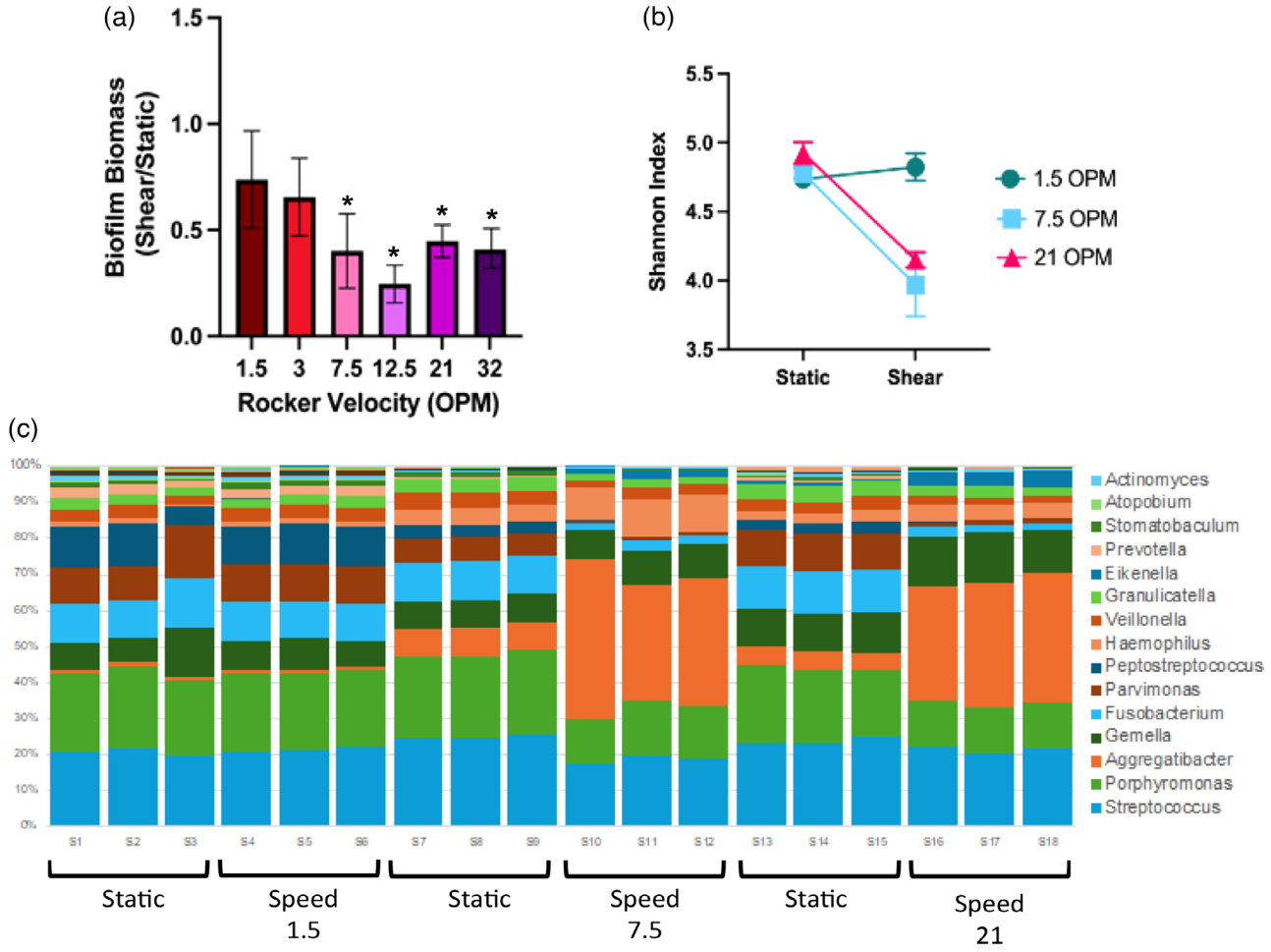

FIGURE 7 Biofilm formation of ex vivo plaque community under fluid shear. (a) Plaque biofilm biomass following growth in Shi media in 12-well plates for 24 h. Data are reported as the mean ± SD ratio of static biofilm formation from ≥3 separate experiments. *p-value ≤ 0.05 as determined by Student's t-test comparing each velocity to static = 100. (b) Alpha diversity analysis using the Shannon diversity index of biofilm communities grown under shear conditions with their static control. (c) Relative abundances of genera detected by 16S rRNA sequencing. The 15 most abundant taxa are labeled. Each column represents one sample. For each speed tested, one set of three static samples was grown and sequenced to account for community composition variation from day to day.

stress levels are relatively low at the center of the well, compared to the periphery. This observation aligns with the accumulation of more biomass at the middle of the well (Figure 3a), and a direct comparison is depicted in Supporting Information Figure S1. Another variable that can impact shear forces is the viscosity of BHI and Shi media, which is lower than that of saliva. Modeling fluid shear in the oral cavity is a complex task and no one model recapitulates the entire intraoral landscape (An et al., 2022; Edlund et al., 2013; Lemus & Valm, 2023; Luo et al., 2022). Furthermore, the shear in the oral cavity cannot be distilled to a single force value or vector (Ong et al., 2018). The rate of flow of saliva across the oral surfaces varies greatly at different sites (Dawes, 2008). Consequently, the thickness and other features of the salivary pellicle on teeth also differ with changes in local conditions (Hannig, 1999). Complicating the features of mucosal salivary films is that the salivary-coated epithelial cells are constantly shedding (Dawes, 2003) and the viscoelastic properties of the mucosa depend on the anatomic location (Lacoste-Ferré et al., 2023). Therefore, we feel that the values generated within our rocker model are reasonable and that our simple model to evaluate the role of complex shear forces is a first informative step toward a more refined analysis.

Consistent with previous studies, we found that as rocker velocity increased, and consequently fluid shear, *S. gordonii* biofilm biomass decreased (Figure 3a). This decrease was largely independent of any decrease in overall bacterial growth (Figure 4). Only at high shear forces did we observe a slight decrease in bacterial growth, which at that point may contribute to the significant loss of biomass (Figure 3a). We evaluated biofilm biomass after 24 h, and therefore it is not yet clear if the decrease in biofilm formed is the result of decreased adhesion or in biofilm development or maintenance.

Under lower fluid shear, we observed a slight increase in biofilm biomass that also appears to be independent of any change in overall bacterial growth (Figures 3 and 4). This suggests the potential for shear-enhanced adhesion and/or extracellular matrix production and subsequent biofilm formation. Several studies have observed

enhanced binding of bacterial cells exposed to shear forces, termed shear-enhanced attachment, although depending on the microbe, the mechanisms may differ (Ebady et al., 2016; Thomas, 2008). *Streptococcus gordonii* has been shown to display shear-enhanced adhesion to saliva and fetuin. This adhesion is dependent on the well-known adhesin Hsa (Ding et al., 2010). The same phenomenon was observed under higher shear conditions in shear-enhanced binding to platelets by *S. gordonii* and *S. sanguinis* (Yakovenko et al., 2018). Shear-enhanced platelet binding was dependent on the adhesins Hsa/GspB for *S. gordonii* and SrpA for *S. sanguinis*. These proteins have been suggested to act as catch-bond adhesins.

There is a growing body of evidence that one way in which bacteria respond to shear forces is through the use of catch-bond adhesins, but proteomic or transcriptomic responses to fluid shear remain few. Existing research shows that the transcriptional response to fluid shear stress varies greatly depending on the study and bacterial species. Our transcriptional analysis of *S. gordonii* exposed to moderate fluid shear identified 50 DEGs, independent of substrates or salivary fractions MUC5B and LDP (Tables 1, S1, and S2). Under shear forces, a higher percentage of genes were down-regulated than up-regulated (46 vs. 4, respectively). One down-regulated cluster was involved in arginine metabolism, commonly used by bacteria to buffer pH and shown to directly impact biofilm formation (Cotter & Hill, 2003; Lindgren et al., 2014; Moleres et al., 2018). Also down-regulated were several clusters related to carbohydrate metabolism. Future studies will investigate the purpose of *S. gordonii* down-regulation of these carbohydrate metabolism genes under shear stress and a potential role in exopolysaccharide production, composition, and utilization as it relates to biofilm maintenance under shear stress. Only four genes were up-regulated under shear and two of them, *rplE* and *rpsQ*, encoding ribosomal proteins and therefore linked to translation.

Of the genes differentially regulated under shear by RNAseq, we selected four genes, *abpB*, *SGO_RS01315*, *SGO_RS02250*, and *SGO_RS06940*, and two non-DEGs encoding adhesin proteins: *mbpA* and *hsa* for further evaluation using quantitative RT-PCR (Figure 6, Table 1). While *mbpA* was not significantly differentially regulated, *hsa* did show significant up-regulation, which reflects similar changes for these genes observed in RNAseq. MbpA has been shown to bind Type I collagen and the salivary mucin MUC5B and aids *S. gordonii* in sensing interaction with MUC5B (Lima et al., 2019, 2022; Nylander et al., 2013). The potential for Hsa and MbpA to function as adhesins required for attachment or biofilm formation under shear stress has yet to be determined; however, a mutant in MbpA displays variable contribution to static, monospecies biofilm formation by *S. gordonii*, while *hsa* deletion significantly reduced biofilm formation (Nairn et al., 2020). For *hsa*, one would not necessarily expect shear-dependent transcriptional regulation since as a catch-bond adhesin, its attachment to the substrate is enhanced by conformational changes induced by shear; however, it is worth further investigation. For the four DEGs from the RNAseq, the quantitative RT-PCR data largely mirrored the RNAseq results (Table 1, Figure 6). *SGO_RS02250*, which was up-regulated under shear, encodes a predicted DNA-binding transcriptional regulator of the YebC/PmpR family. These regulators have been tied to the regulation of quorum sensing, proteolytic systems, DNA repair, and virulence factors in other organisms (Brown et al., 2017; Byrne et al., 2014; Liang et al., 2008; L. Wei et al., 2018; Zhang et al., 2020). Further studies need to be completed to investigate further any role for this regulator in the response to fluid flow.

We also evaluated three down-regulated genes: *abpB*, *SGO_RS01315*, and *SGO_RS06940*. AbpB is a functional C69 family dipeptidyl-dipeptidase, and while studies suggest it may be involved in multispecies biofilm formation, it is not required for monospecies *S. gordonii* biofilm formation (Nairn et al., 2020). *SGO_RS01315* is a predicted polyamine/amino acid transporter (PotE, putrescine/ornithine antiporter) though its function remains to be biochemically validated. The other genes related to polyamine transport and utilization (*potABCD*) were not differentially expressed. The role of polyamines in biofilm formation varies depending on the organism (Nanduri & Swiatlo, 2021). Last, *SGO_RS06940* is a predicted cell wall protein annotated as an S15 family X-prolyl dipeptidylpeptidase with homology to PepX of *Lactobacillus* (Kieliszek et al., 2021). A second PepX homolog (SGO_0234) is also found in *S. gordonii;* however, we did not observe differential expression of this gene (Goldstein et al., 2001). All three of these genes are potentially involved in amino acid transport and metabolism, systems whose roles in biofilm formation under shear forces have yet to be evaluated and are the goal of future studies.

The effect of shear forces on our ex vivo plaque model was similar to what we saw with *S. gordonii*: As fluid shear increased, biofilm biomass decreased (Figure 7a). To some extent, this contradicts Fernandez et al.'s (2016) observation of no change or a slight increase in biomass when different oral biofilms were exposed to increasing fluid shear (0.1, 0.2, and 0.4 dyn/cm^2, equivalent to 0.01, 0.02, and 0.04 Pa, respectively). It is worth noting that the growth media and method used to generate shear forces differed significantly between our study and Fernandez et al. (2016), which could have easily contributed to the seemingly opposite biofilm biomass results.

When it comes to community composition, our 16S sequencing data allowed us to assign genus information to our taxa, providing greater insight into community composition changes in response to fluid shear. In our studies, no difference in community composition was observed at our lowest OPM (1.5), when compared to the static biofilm (Figure 7b,c), which is perhaps expected given the low amount of shear forces experienced by these biofilms (Figure 2). At higher OPM (7.5 and 21), however, we observed a decrease in the overall community composition when compared to static biofilms, with a notable decrease in the abundance of obligate anaerobic genera such as *Porphyromonas*, *Fusobacterium*, and *Parvimonas*, and an increase in the abundance of the facultative anaerobic genera *Aggregatibacter* and *Hemophilus*. Given the rocker model used in this study and our incubation condition (5% CO_2), it is possible that one of the consequences of increasing OPM is an increase in the oxygen tension in the media, thus affecting the growth of strict anaerobic bacteria. It would be interesting to see what happens to the community composition if we were able to replicate this experiment inside an anaerobic chamber. Strikingly, *Streptococcus* representation was minimally affected under shear in our ex vivo model,

suggesting that in the context of a multispecies setting, the effect of fluid shear on streptococci such as *S. gordonii* might be diminished.

Overall, we have developed a simple model of fluid shear and evaluated biofilm biomass and the composition of oral bacterial biofilms. We also used this model to probe the transcriptional response of *S. gordonii* to fluid shear, providing insights into factors required by oral bacteria to form plaque communities in the oral environment and bacterial adaptation to fluid shear. These studies can inform how we study biofilms under authentic environmental conditions and, in many cases, treat or prevent biofilm formation in patients.

ACKNOWLEDGMENTS

This work was supported by the National Institute of Dental and Craniofacial Research (NIDCR) R01 DE025618 awarded to M. C. Herzberg, K08 DE027705 and R03 DE031337 awarded to B. P. Lima. J. Yang and G. Wei are supported by the National Science Foundation (NSF) CAREER Award 2236497. MUC5B and LDP salivary fractions were kindly provided by Claes Wickström at Malmö University, Malmö, Sweden. The authors would like to thank members of the Herzberg and Lima laboratories for their thoughtful recommendations during the preparation of this manuscript.

CONFLICT OF INTEREST STATEMENT

The other authors have stated that there are no conflicts of interest.

DATA AVAILABILITY STATEMENT

The data that support the findings of this study are available from the corresponding author upon reasonable request.

ORCID

Brittany L. Nairn https://orcid.org/0000-0003-1311-7294
Bruno P. Lima https://orcid.org/0000-0003-4619-4712
Judy Q. Yang https://orcid.org/0000-0001-6272-1266
Guanju Wei https://orcid.org/0000-0001-5511-9242

REFERENCES

Aas, J. A., Paster, B. J., Stokes, L. N., Olsen, I., & Dewhirst, F. E. (2005). Defining the normal bacterial flora of the oral cavity. *Journal of Clinical Microbiology*, *43*(11), 5721–5732. https://doi.org/10.1128/JCM.43.11.5721-5732.2005

Akhlaghi, A. H. A., & Hamouda, A. A. (2013). Evaluation of level set and phase field methods in modeling two phase flow with viscosity contrast through dual-permeability porous medium. *International Journal of Multiphase Flow*, *52*, 22–34. https://doi.org/10.1016/j.ijmultiphaseflow.2012.12.006

Alsharif, G., Ahmad, S., Islam, M. S., Shah, R., Busby, S. J., & Krachler, A. M. (2015). Host attachment and fluid shear are integrated into a mechanical signal regulating virulence in *Escherichia coli* O157:H7. *Proceedings of the National Academy of Sciences of the United States of America*, *112*(17), 5503–5508. https://doi.org/10.1073/pnas.1422986112

An, S., Hull, R., Metris, A., Barrett, P., Webb, J. S., & Stoodley, P. (2022). An in vitro biofilm model system to facilitate study of microbial communities of the human oral cavity. *Letters in Applied Microbiology*, *74*(3), 302–310. https://doi.org/10.1111/lam.13618

Back, C. R., Sztukowska, M. N., Till, M., Lamont, R. J., Jenkinson, H. F., Nobbs, A. H., & Race, P. R. (2017). The *Streptococcus gordonii* adhesin CshA protein binds host fibronectin via a catch-clamp mechanism. *The Journal of Biological Chemistry*, *292*(5), 1538–1549. https://doi.org/10.1074/jbc.M116.760975

Baty, J. J., Stoner, S. N., & Scoffield, J. A. (2022). Oral commensal streptococci: Gatekeepers of the oral cavity. *Journal of Bacteriology*, *204*(11), e0025722–e0025722. https://doi.org/10.1128/jb.00257-22

Bolyen, E., Rideout, J. R., Dillon, M. R., Bokulich, N. A., Abnet, C. C., Al-Ghalith, G., Alexander, H., Alm, E. J., Arumugam, M., Asnicar, F., Bai, Y., Bisanz, J. E., Bittinger, K., Brejnrod, A., Brislawn, C. J., Brown, C. T., Callahan, B. J., Caraballo-Rodríguez, A. M., Chase, J., … Caporaso, J. G. (2019). Reproducible, interactive, scalable and extensible microbiome data science using QIIME 2. *Nature Biotechnology*, *37*(8), 852–857. https://doi.org/10.1038/s41587-019-0209-9

Brown, L., Villegas, J. M., Elean, M., Fadda, S., Mozzi, F., Saavedra, L., & Hebert, E. M. (2017). YebC, a putative transcriptional factor involved in the regulation of the proteolytic system of *Lactobacillus*. *Scientific Reports*, *7*(1), 8579. https://doi.org/10.1038/s41598-017-09124-1

Byrne, R. T., Chen, S. H., Wood, E. A., Cabot, E. L., & Cox, M. M. (2014). *Escherichia coli* genes and pathways involved in surviving extreme exposure to ionizing radiation. *Journal of Bacteriology*, *196*(20), 3534–3545. https://doi.org/10.1128/JB.01589-14

Callahan, B. J., McMurdie, P. J., Rosen, M. J., Han, A. W., Johnson, A. J. A., & Holmes, S. P. (2016). DADA2: High-resolution sample inference from illumina amplicon data. *Nature Methods*, *13*(7), 581–583. https://doi.org/10.1038/nmeth.3869

Christersson, C. E., Glantz, P. O., & Baier, R. E. (1988). Role of temperature and shear forces on microbial detachment. *Scandinavian Journal of Dental Research*, *96*(2), 91–98. https://doi.org/10.1111/j.1600-0722.1988.tb01413.x

COMSOL. (2015). *CFD module user's guide*. https://doc.comsol.com/5.2/doc/com.comsol.help.cfd/CFDModuleUsersGuide.pdf

Cotter, P. D., & Hill, C. (2003). Surviving the acid test: Responses of gram-positive bacteria to low pH. *Microbiology and Molecular Biology Reviews*, *67*(3), 429–453. https://doi.org/10.1128/MMBR.67.3.429-453.2003

Cremer, J., Segota, I., Yang, C., Arnoldini, M., Sauls, J. T., Zhang, Z., Gutierrez, E., Groisman, A., & Hwa, T. (2016). Effect of flow and peristaltic mixing on bacterial growth in a gut-like channel. *Proceedings of the National Academy of Science of the United States of America*, *113*(41), 11414–11419. https://doi.org/10.1073/pnas.1601306113

Dawes, C. (2003). Estimates, from salivary analyses, of the turnover time of the oral mucosal epithelium in humans and the number of bacteria in an edentulous mouth. *Archives of Oral Biology*, *48*(5), 329–336. https://doi.org/10.1016/s0003-9969(03)00014-1

Dawes, C. (2008). Salivary flow patterns and the health of hard and soft oral tissues. *Journal of the American Dental Association (1939)*, *139*, 18S–24S. https://doi.org/10.14219/jada.archive.2008.0351

Diaz, P. I., Chalmers, N. I., Rickard, A. H., Kong, C., Milburn, C. L., Palmer, R. J. J., & Kolenbrander, P. E. (2006). Molecular characterization of subject-specific oral microflora during initial colonization of enamel. *Applied and Environmental Microbiology*, *72*(4), 2837–2848. https://doi.org/10.1128/AEM.72.4.2837-2848.2006

Ding, A. M., Palmer, R. J. J., Cisar, J. O., & Kolenbrander, P. E. (2010). Shear-enhanced oral microbial adhesion. *Applied and Environmental Microbiology*, *76*(4), 1294–1297. https://doi.org/10.1128/AEM.02083-09

Dingemans, J., Monsieurs, P., Yu, S., Crabbé, A., Förstner, K. U., Malfroot, A., Cornelius, P., & Van Houdt, R. (2016). Effect of shear stress on *Pseudomonas aeruginosa* isolated from the cystic fibrosis lung. *mBio*, *7*(4), e00813–816. https://doi.org/10.1128/mBio.00813-16

Ebady, R., Niddam, A. F., Boczula, A. E., Kim, Y. R., Gupta, N., Tang, T. T., Odisho, T., Zhi, H., Simmons, C. A., Skare, J. T., & Moriarty, T. (2016). Biomechanics of *Borrelia burgdorferi* vascular interactions. *Cell Reports*, *16*(10), 2593–2604. https://doi.org/10.1016/j.celrep.2016.08.013

Edlund, A., Yang, Y., Hall, A. P., Guo, L., Lux, R., He, X., Nelson, K. E., Nealson, K. H., Yooseph, S., Shi, W., & McLean, J. S. (2013). An *in vitro* biofilm model

system maintaining a highly reproducible species and metabolic diversity approaching that of the human oral microbiome. *Microbiome*, *1*(1), 25. https://doi.org/10.1186/2049-2618-1-25

Fernández, C. E., Aspiras, M. B., Dodds, M. W., González-Cabezas, C., & Rickard, A. H. (2016). The effect of inoculum source and fluid shear force on the development of in vitro oral multispecies biofilms. *Journal of Applied Microbiology*, *122*(3), 796–808. https://doi.org/10.1111/jam.13376

Goldstein, J. M., Banbula, A., Kordula, T., Mayo, J. A., & Travis, J. (2001). Novel extracellular x-prolyl dipeptidyl-peptidase (DPP) from *Streptococcus gordonii* FSS2: An emerging subfamily of viridans streptococcal x-prolyl DPPs. *Infection and Immunity*, *69*(9), 5494–5501. https://doi.org/10.1128/IAI.69.9.5494-5501.2001

Hall, J. W., Lima, B. P., Herbomel, G. G., Gopinath, T., McDonald, L., Shyne, M. T., Lee, J. K., Kreth, J., Ross, K. F., Veglia, G., & Herzberg, M. C. (2019). An intramembrane sensory circuit monitors sortase A-mediated processing of streptococcal adhesins. *Science Signaling*, *12*(580), eaas9941. https://doi.org/10.1126/scisignal.aas9941

Hannig, M. (1999). Ultrastructural investigation of pellicle morphogenesis at two different intraoral sites during a 24-h period. *Clinical Oral Investigations*, *3*(2), 88–95. https://doi.org/10.1007/s007840050084

Illumina. (2020). BCL Convert [Computer software]. Illumina.

Jakubovics, N. S., Strömberg, N., van Dolleweerd, C. J., Kelly, C. G., & Jenkinson, H. F. (2005). Differential binding specificities of oral streptococcal antigen I/II family adhesins for human or bacterial ligands. *Molecular Microbiology*, *55*(5), 1591–1605. https://doi.org/10.1111/j.1365-2958.2005.04495.x

Kieliszek, M., Pobiega, K., Piwowarek, K., & Kot, A. M. (2021). Characteristics of the proteolytic enzymes produced by lactic acid bacteria. *Molecules*, *26*(7), 1858. https://doi.org/10.3390/molecules26071858

Kim, M. K., Ingremeau, F., Zhao, A., Bassler, B. L., & Stone, H. A. (2016). Local and global consequences of flow on bacterial quorum sensing. *Nature Microbiology*, *1*(1), 15005. https://doi.org/10.1038/nmicrobiol.2015.5

Kindblom, C., Davies, J. R., Herzberg, M. C., Svensater, G., & Wickstrom, C. (2012). Salivary proteins promote proteolytic activity in *Streptococcus mitis* biovar 2 and *Streptococcus mutans*. *Molecular Oral Microbiology*, *27*(5), 362–372. https://doi.org/10.1111/j.2041-1014.2012.00650.x

Kostenko, V., Salek, M. M., Sattari, P., & Martinuzzi, R. J. (2010). *Staphylococcus aureus* biofilm formation and tolerance to antibiotics in response to oscillatory shear stresses of physiological levels. *FEMS Immunology and Medical Microbiology*, *59*(3), 421–431. https://doi.org/10.1111/j.1574-695X.2010.00694.x

Lacoste-Ferré, M., Ober, C., & Samouillan, V. (2023). Viscoelastic behavior of oral mucosa. A rheological study using small-amplitude oscillatory shear tests. *Journal of the Mechanical Behavior of Biomedical Materials*, *143*, 105898. https://doi.org/10.1016/j.jmbbm.2023.105898

Lecuyer, S., Rusconi, R., Shen, Y., Forsyth, A., Vlamakis, H., Kolter, R., & Stone, H. A. (2011). Shear stress increases the residence time of adhesion of *Pseudomonas aeruginosa*. *Biophysical Journal*, *100*(2), 341–350. https://doi.org/10.1016/j.bpj.2010.11.078

Lemus, A. A., & Valm, A. M. (2023). In vitro dental plaque culture model for biofilm structural analyses. *Current Protocols*, *3*(10), e902. https://doi.org/10.1002/cpz1.902

Liang, H., Li, L., Dong, Z., Surette, M. G., & Duan, K. (2008). The YebC family protein PA0964 negatively regulates the *Pseudomonas aeruginosa* quinolone signal system and pyocyanin production. *Journal of Bacteriology*, *190*(18), 6217–6227. https://doi.org/10.1128/JB.00428-08

Lima, B. P., Kho, K., Nairn, B. L., Davies, J. R., Svensäter, G., Chen, R., Steffes, A., Vreeman, G. W., Meredith, T. C., & Herzberg, M. C. (2019). *Streptococcus gordonii* type I lipoteichoic acid contributes to surface protein biogenesis. *mSphere 4*, *4*(6), e00814–819. https://doi.org/10.1128/mSphere.00814-19

Lima, B. P., Davies, J. R., Wickström, C., Johnstone, K. F., Hall, J. W., Svensater, G., & Herzberg, M. C. (2022). *Streptococcus gordonii* poised for glycan feeding through a MUC5B-discriminating, lipoteichoic acid-mediated outside-in signaling circuit. *Journal of Bacteriology*, *204*(6), e0011822–22. https://doi.org/10.1128/jb.00118-22

Lindgren, J. K., Thomas, V. C., Olson, M. E., Chaudhari, S. S., Nuxoll, A. S., Schaeffer, C. R., Lindgren, K. E., Jones, J., Zimmerman, M. C., Dunman, P. M., Bayles, K. W., & Fey, P. D. (2014). Arginine deiminase in *Staphylococcus epidermidis* functions to augment biofilm maturation through pH homeostasis. *Journal of Bacteriology*, *196*(12), 2277–2289. https://doi.org/10.1128/JB.00051-14

Liu, Y., & Tay, J. (2002). The essential role of hydrodynamic shear force in the formation of biofilm and granular sludge. *Water Research*, *36*(7), 1653–1665. https://doi.org/10.1016/s0043-1354(01)00379-7

Luo, T. L., Vanek, M. E., Gonzalez-Cabezas, C., Marrs, C. F., Foxman, B., & Rickard, A. H. (2022). In vitro model systems for exploring oral biofilms: From single-species populations to complex multi-species communities. *Journal of Applied Microbiology*, *132*(2), 855–871. https://doi.org/10.1111/jam.15200

Martin, M. (2011). Cutadapt removes adapter sequences from high-throughput sequencing reads. *EMBnet Journal*, *17*(1), 10–12. https://doi.org/10.14806/ej.17.1.200

Moleres, J., Fernández-Calvet, A., Ehrlich, R. L., Marti, S., Pérez-Regidor, L., Euba, B., Rodríguez-Arce, I., Balashov, S., Cuevas, E., Liñares, J., Ardanuy, C., Martín-Santamaría, S., Ehrlich, G. D., Mell, J. C., & Garmendia, J. (2018). Antagonistic pleiotropy in the bifunctional surface protein FadL (OmpP1) during adaptation of *Haemophilus influenzae* to chronic lung infection associated with chronic obstructive pulmonary disease. *mBio*, *9*(5), e01176–18. https://doi.org/10.1128/mBio.01176-18

Nairn, B. L., Lee, G. T., Chumber, A. K., Steck, P. R., Mire, M. O., Lima, B. P., & Herzberg, M. C. (2020). Uncovering roles of *Streptococcus gordonii* SrtA-processed proteins in the biofilm lifestyle. *Journal of Bacteriology*, *203*(2), e00544–20. https://doi.org/10.1128/JB.00544-20

Nanduri, B., & Swiatlo, E. (2021). The expansive effects of polyamines on the metabolism and virulence of *Streptococcus pneumoniae*. *Pneumonia*, *13*(1), 4. https://doi.org/10.1186/s41479-021-00082-x

Nobbs, A. H., Zhang, Y., Khammanivong, A., & Herzberg, M. C. (2007). *Streptococcus gordonii* Hsa environmentally constrains competitive binding by *Streptococcus sanguinis* to saliva-coated hydroxyapatite. *Journal of Bacteriology*, *189*(8), 3106–3114. https://doi.org/10.1128/JB.01535-06

Nylander, A., Svensater, G., Senadheera, D. B., Cvitkovitch, D. G., Davies, J. R., & Persson, K. (2013). Structural and functional analysis of the N-terminal domain of the *Streptococcus gordonii* adhesin Sgo0707. *PloS One*, *8*(5), e63768. https://doi.org/10.1371/journal.pone.0063768

Ong, J. J., Steele, C. M., & Duizer, L. M. (2018). Challenges to assumptions regarding oral shear rate during oral processing and swallowing based on sensory testing with thickened liquids. *Food Hydrocolloids*, *84*, 173–180. https://doi.org/10.1016/j.foodhyd.2018.05.043

Pappelbaum, K. I., Gorzelanny, C., Grässle, S., Suckau, J., Laschke, M. W., Bischoff, M., Bauer, C., Schorpp-Kistner, M., Weidenmaier, C., Schneppenheim, R., Obser, T., Sinha, B., & Schneider, S. W. (2013). Ultralarge von Willebrand factor fibers mediate luminal *Staphylococcus aureus* adhesion to an intact endothelial cell layer under shear stress. *Circulation*, *128*(1), 50–59. https://doi.org/10.1161/CIRCULATIONAHA.113.002008

Paramonova, E., Kalmykowa, O. J., van der Mei, H. C., Busscher, H. J., & Sharma, P. K. (2009). Impact of hydrodynamics on oral biofilm strength. *Journal of Dental Research*, *88*(10), 922–926. https://doi.org/10.1177/0022034509344569

Prakobphol, A., Burdsal, C. A., & Fisher, S. J. (1995). Quantifying the strength of bacterial adhesive interactions with salivary glycoproteins. *Journal of Dental Research*, *74*(5), 1212–1218. https://doi.org/10.1177/00220345950740051101

Rodesney, C. A., Roman, B., Dhamani, N., Cooley, B. J., Katira, P., Touhami, A., & Gordon, V. D. (2017). Mechanosensing of shear by *Pseudomonas aeruginosa* leads to increased levels of the cyclic-di-GMP signal

initiating biofilm development. *Proceedings of the National Academy of Sciences*, *114*(23), 5906–5911. https://doi.org/10.1073/pnas.1703255114

Rognes, T., Flouri, T., Nichols, B., Quince, C., & Mahé, F. (2016). VSEARCH: A versatile open source tool for metagenomics. *PeerJ*, *4*, e2584. https://doi.org/10.7717/peerj.2584

Ruhl, S., Sandberg, A. L., & Cisar, J. O. (2004). Salivary receptors for the proline-rich protein-binding and lectin-like adhesins of oral actinomyces and streptococci. *Journal of Dental Research*, *83*(6), 505–510. https://doi.org/10.1177/154405910408300614

Saavedra, F. M., Pelepenko, L. E., Boyle, W. S., Zhang, A. A., Staley, C. C., Herzberg, M. C., Marciano, M. A., & Lima, B. P. (2022). In vitro physicochemical characterization of five root canal sealers and their influence on an ex vivo oral multi-species biofilm community. *International Endodontic Journal*, *55*(7), 772–783. https://doi.org/10.1111/iej.13742

Sanfilippo, J. E., Lorestani, A., Koch, M. D., Bratton, B. P., Siryaporn, A., Stone, H. A., & Gitai, Z. (2019). Microfluidic-based transcriptomics reveal force-independent bacterial rheosensing. *Nature Microbiology*, *4*(8), 1274–1281. https://doi.org/10.1038/s41564-019-0455-0

Saunders, K. A., & Greenman, J. (2000). The formation of mixed culture biofilms of oral species along a gradient of shear stress. *Journal of Applied Microbiology*, *89*(4), 564–572. https://doi.org/10.1046/j.1365-2672.2000.01148.x

Schollin, J. (1988). Adherence of alpha-hemolytic streptococci to human endocardial, endothelial and buccal cells. *Acta Paediatrica*, *77*(5), 705–710. https://doi.org/10.1111/j.1651-2227.1988.tb10734.x

Sharma, P. K., Gibcus, M. J., van der Mei, H. C., & Busscher, H. J. (2005). Influence of fluid shear and microbubbles on bacterial detachment from a surface. *Applied and Environmental Microbiology*, *71*(7), 3668–3673. https://doi.org/10.1128/AEM.71.7.3668-3673.2005

Siqueira, W. L., Zhang, W., Helmerhorst, E. J., Gygi, S. P., & Oppenheim, F. G. (2007). Identification of protein components in in vivo human acquired enamel pellicle using LC-ESI-MS/MS. *Journal of Proteome Research*, *6*(6), 2152–2160. https://doi.org/10.1021/pr060580k

Thomas, W. (2008). Catch bonds in adhesion. *Annual Review of Biomedical Engineering*, *10*, 39–57. https://doi.org/10.1146/annurev.bioeng.10.061807.160427

Thomas, W. E., Trintchina, E., Forero, M., Vogel, V., & Sokurenko, E. V. (2002). Bacterial adhesion to target cells enhanced by shear force. *Cell*, *109*(7), 913–923. https://doi.org/10.1016/s0092-8674(02)00796-1

Thomen, P., Robert, J., Monmeyran, A., Bitbol, A., Douarche, C., & Henry, N. (2017). Bacterial biofilm under flow: First a physical struggle to stay, then a matter of breathing. *PLoS ONE*, *12*(4), e0175197. https://doi.org/10.1371/journal.pone.0175197

Weaver, W. M., Dharmaraja, S., Milisavljevic, V., & Di Carlo, D. (2011). The effects of shear stress on isolated receptor-ligand interactions of *Staphylococcus epidermidis* and human plasma fibrinogen using molecularly patterned microfluidics. *Lab on a Chip*, *11*(5), 883–889. https://doi.org/10.1039/c0lc00414f

Wei, L., Wu, Y., Qiao, H., Xu, W., Zhang, Y., Liu, X., & Wang, Q. (2018). YebC controls virulence by activating T3SS gene expression in the pathogen *Edwardsiella piscicida*. *FEMS Microbiology Letters*, *365*(14), 10. https://doi.org/10.1093/femsle/fny137

Wei, G., & Yang, J. Q. (2023). Impacts of hydrodynamic conditions and microscale surface roughness on the critical shear stress to develop and thickness of early-stage *Pseudomonas putida* biofilms. *Biotechnology and Bioengineering*, *120*(7), 1797–1808. https://doi.org/10.1002/bit.28409

Weston, M. W., LaBorde, D. V., & Yoganathan, A. P. (1999). Estimation of the shear stress on the surface of an aortic valve leaflet. *Annals of Biomedical Engineering*, *27*(4), 572–579. https://doi.org/10.1114/1.199

Yakovenko, O., Nunez, J., Bensing, B., Yu, H., Mount, J., Zeng, J., Hawkins, J., Chen, X., Sullam, P. M., & Thomas, W. (2018). Serine-rich repeat adhesins mediate shear-enhanced streptococcal binding to platelets. *Infection and Immunity*, *86*(6), e00160–18. https://doi.org/10.1128/iai.00160-18

Yakovenko, O., Sharma, S., Forero, M., Tchesnokova, V., Aprikian, P., Kidd, B., Mach, A., Vogel, V., Sokurenko, E., & Thomas, W. E. (2008). FimH forms catch bonds that are enhanced by mechanical force due to allosteric regulation. *The Journal of Biological Chemistry*, *283*(17), 11596–11605. https://doi.org/10.1074/jbc.M707815200

Yao, Y., Berg, E. A., Costello, C. E., Troxler, R. F., & Oppenheim, F. G. (2003). Identification of protein components in human acquired enamel pellicle and whole saliva using novel proteomics approaches. *The Journal of Biological Chemistry*, *278*(7), 5300–5308. https://doi.org/10.1074/jbc.M206333200

Zhang, Y., Chen, T., Raghunandanan, S., Xiang, X., Yang, J., Liu, Q., Edmondson, D. G., Norris, S. J., Yang, X. F., & Lou, Y. (2020). YebC regulates variable surface antigen VlsE expression and is required for host immune evasion in *Borrelia burgdorferi*. *PLOS Pathogens*, *16*(10), e1008953. https://doi.org/10.1371/journal.ppat.1008953

SUPPORTING INFORMATION

Additional supporting information can be found online in the Supporting Information section at the end of this article.

How to cite this article: Nairn, B. L., Lima, B. P., Chen, R., Yang, J. Q., Wei, G., Chumber, A. K., & Herzberg, M. C. (2024). Effects of fluid shear stress on oral biofilm formation and composition and the transcriptional response of *Streptococcus gordonii*. *Molecular Oral Microbiology*, 1–14. https://doi.org/10.1111/omi.12481